Design of Sideband Separation SIS Mixer for 3 mm Band

V. Vassilev and V. Belitsky
Onsala Space Observatory, Chalmers University of Technology

ABSTRACT

As a part of Onsala development of a single sideband mixer for ALMA band 7 (275-370 GHz), we present the design of a prototype sideband separation mixer for 85-115 GHz. The mixer is designed using a quadrature scheme with two identical DSB SIS mixers pumped by a local oscillator (LO) with 90° phase difference. The mixer employs a new device, a double-probe coupler, which splits the input RF signal and provides transition from a waveguide to a microstrip line, allowing the integration of all mixer components on the same compact substrate and thus ensure a high degree of similarity in the SIS junction performance and the geometry of all the mixer elements including integrated tuning circuitry. The RF and the LO power are coupled on the substrate by using microstrip directional coupler; the remaining LO power at the idle port of the coupler is terminated by unbiased (or weakly biased) SIS junction acting as a lumped load. To obtain feasible dimensions of the LO directional coupler and the SIS tuning circuitry the mixer is designed using two types of dielectric: 150 μm thick crystal quartz substrate and two layers (400 nm and 200 nm) of sputtered SiO_2. The presence of the two dielectrics (quartz and SiO_2) requires step in the ground plane, which is achieved by using a choke structure as a virtual ground [1].
We present the design of all the mixer components, detailed simulation results using High Frequency Structure Simulator and measurements of the double probe coupler.

INTRODUCTION

In [2] Jewell and Mangum examine in details single versus double sideband operation in terms of the signal-to-noise ratio and optimum receiver performance. They found that SSB observations are more efficient not only for spectroscopic observations in one sideband, but even if spectral lines of interest are present in both sidebands. With SIS mixer noise temperature approaching level of 2-5 times the quantum noise, the noise performance of a double-side band (DSB) super-heterodyne receiver can be limited by the atmospheric noise fed into the system via the image band. A separation of the atmospheric noise introduced by the image band can improve the sensitivity of a SSB receiver up to a factor of two over the DSB receiver with balanced sideband gains [4].
A quadrature scheme with two identical DSB SIS mixers pumped by a local oscillator (LO) with 90° phase difference as shown in Figure 1 does not use any RF filter components and has been demonstrated for mm-wave band [3, 4].

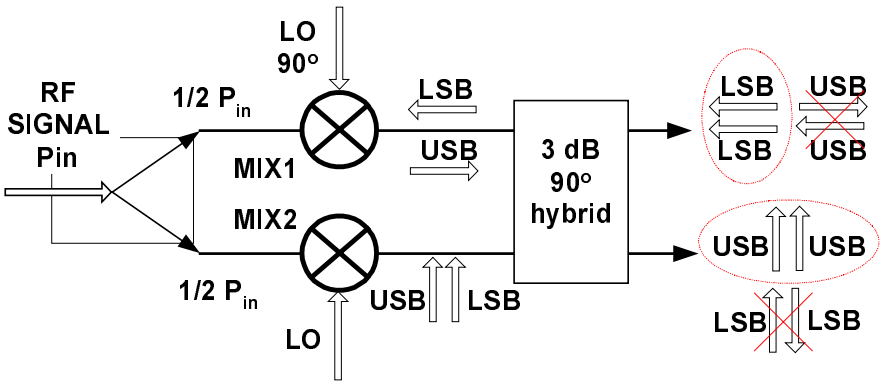

Figure 1 Block diagram of the sideband separation mixer. The crossed out items at the hybrid outputs are the rejected sidebands (180° phase difference).

The RF and the LO amplitude and phase *balance* at the two mixers is the limiting factor [5] in the separation of the image band (more than 10 dB is a typical specification).

MIXER DESCRIPTION

The whole mixer circuitry is design on a single crystal quartz substrate 9mm/ 0.7mm/ 150µm as shown in Figure 2.

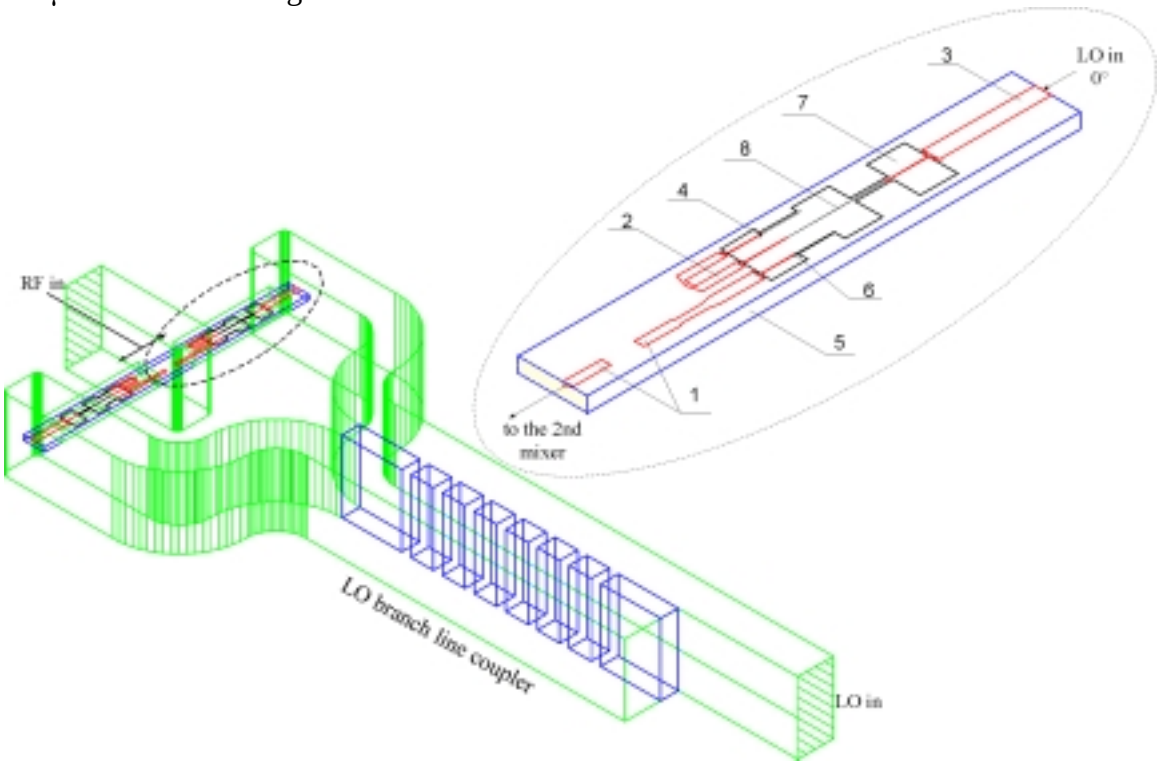

Figure 2 Layout of the sideband separation mixer. 1- double probe 3 dB coupler, 2- 15dB LO directional coupler, 3- LO waveguide to microstrip transition, 4- SIS junction as an absorbing load, 5- crystal quartz substrate, 6- SIS mixer junction, 7- choke structure, 8- 3 sections transformer matching the LO probe to the LO injection coupler.

The substrate is coupled to the RF waveguide via a double-probe 3dB coupler (1). A waveguide branch line coupler provides 90° phase shift and splits the LO power which is then coupled at the ends of the substrate. Three section transformer (8) matches the impedance of the LO probe (3) to the LO injection coupler (2). To keep the signal path loss small the LO power is coupled to the RF via –15dB directional coupler (2). SIS junction (4) is used as a load for the idle ports of the substrate LO coupler to terminate the remaining LO power.

Two types of transmission line media are used: microstrip lines (the lines linked to 1, 2 and 3 from Figure 2) which use the 150μm crystal quartz substrate as dielectric and 'narrow' microstrip lines (the lines located above the choke 7) which are placed on the top of a thin sputtered SiO_2 layer. To increase the upper limit of the attainable impedances of SiO_2 based line, two layers of SiO_2 are used- 200nm layer, which is placed over the last sections of the choke and accommodates the SIS junctions and a second 200nm layer (on top of the first one) over the middle choke sections allowing increase in the line impedance by a factor of 2 up to ≈ 25 Ω.

THE DOUBLE-PROBE COUPLER

In attempt to simplify the design by combining the low-loss, wide band power division with the waveguide to microstrip transition, we suggest a device where a double-probe structure is coupled to the E-field in a waveguide as shown in Figure 3. The probes split the input RF signal over a frequency band limited by the dominant mode of the waveguide and simultaneously provide transition from waveguide to microstrip line for easy integration with the associated mixer circuitry [6].

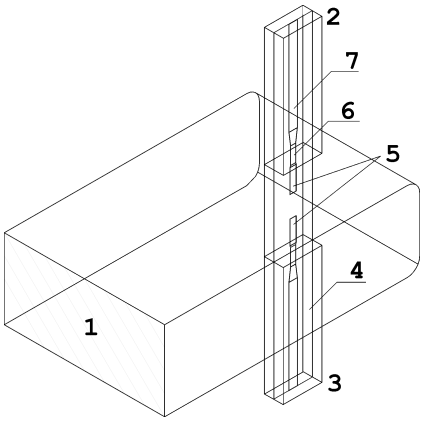

Figure 3 Waveguide to microstrip power divider. 1 – the input port, 2,3 – the output ports, 4 – channel with the substrate, 5 – probes, 6 – high impedance line, 7 – output microstrip line.

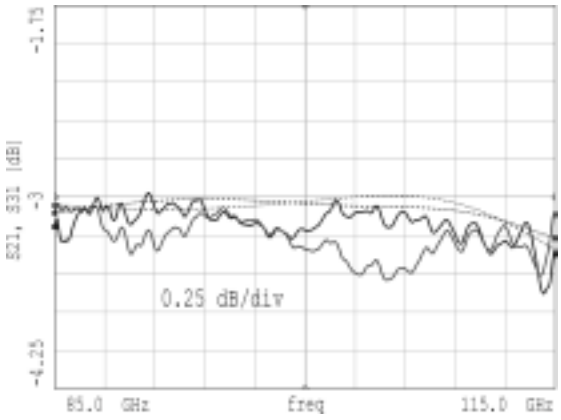

Figure 4 Measured transmission magnitude of the power divider (solid lines) and the simulated transmission (dashed lines).

The transmission S_{21} and S_{31} were measured between 85-115 GHz and are plotted in Figure 4, the typical total loss is ≈0.3dB over 30% of bandwidth. In this measurement

only response calibration was performed, the observed amplitude asymmetry is ≤ 0.3 dB and is likely caused by the interaction between the system's source and loads mismatch. The double probe coupler is a perfect phase-splitter, since the E-field vector oscillates in the direction parallel to the probes; phase difference of 180° is introduced between the output ports for all frequencies of the waveguide dominant mode. Thus the suggested power divider provides perfect phase symmetry. Good amplitude symmetry is observed as long as the output ports are terminated with identical loads. The power divider transducer power gain was examined for different values of possible loads mismatch and the resulting asymmetry is compared to that of the ideal Wilkinson in [6], it was shown that for small load impedance deviations Z_L/Z_0 the asymmetry of the suggested power divider converges to the one of the ideal Wilkinson divider.

LO DIRECTIONAL COUPLER

A number of attempts were made to design a LO injection directional coupler by using the SiO_2 as transmission medium. However due to the small dielectric thickness, the gap required between the coupled lines appears to be critically small even if periodic capacitive coupling is introduced on top of the lines. To ease the processing requirements the LO injection coupler was designed using the crystal quartz substrate as a dielectric which also facilitates its connection to the double probe coupler. The LO coupler together with the power divider is shown in Figure 5.

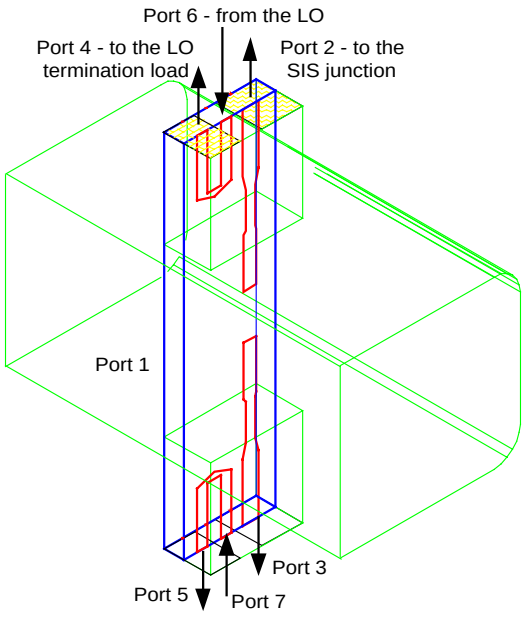

Figure 5 LO injection directional coupler together with the power divider. Port 1 is the RF waveguide input, ports 2, 3 are connected to the SIS junctions via a λ/4 transformer section, the LO power is applied at ports 6 and 7, ports 4 and 5 are connected to the LO termination load (unbiased SIS junctions).

The transmission lines were designed as wide as possible in order to decrease the impedance at the ports to ease the matching to the SIS junctions. The resultant 7 ports

structure was analyzed using HFSS simulator [8], and the simulated performance is shown in Figure 6. The shape of the line that provides 180° bend in the LO path was optimized to minimize the reflection caused by the 'sharp' bend.

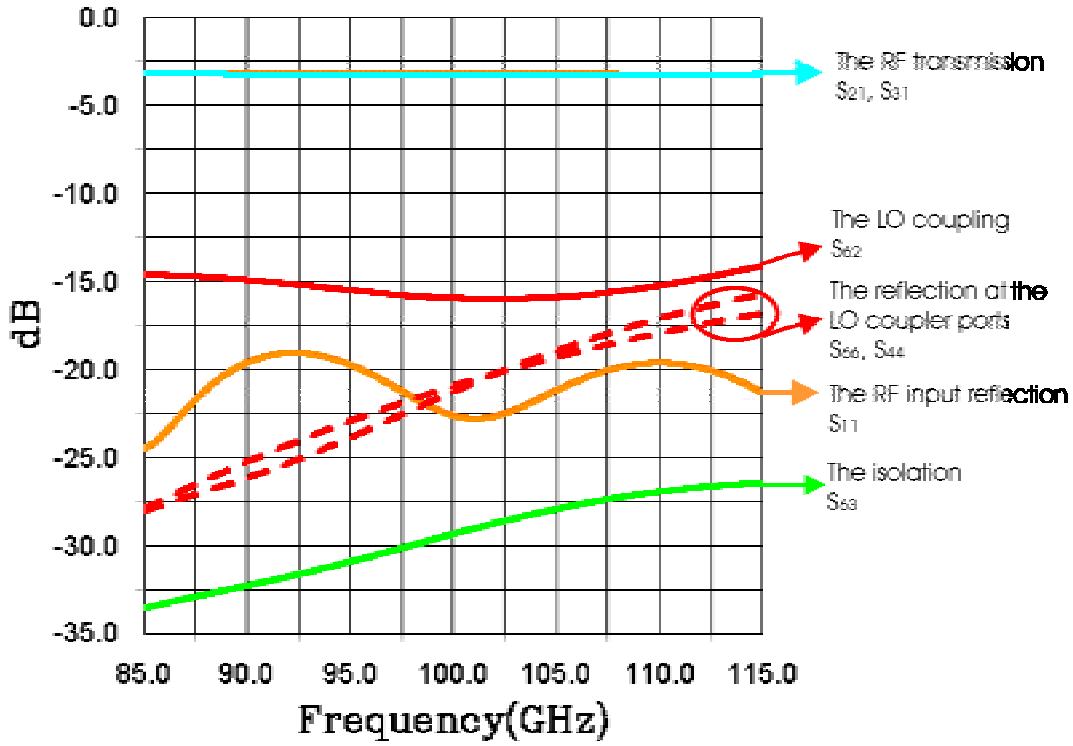

Figure 6 Simulated performance of the RF power divider and LO injection coupler.

The LO to RF coupling is nearly constant –15dB, the return loss at all the ports is > 17 dB and the directivity is > 14dB.

CHOKE

Incorporating the two types of dielectric– 150 μm crystal quartz substrate and the two layers of SiO_2 (200nm and 400 nm) for the lines surrounding the SIS junctions requires transition between the two ground planes. More effective step in the ground can be achieved by shaping the upper ground plane as a 'choke' or band-stop filter as suggested by [1]. This idea is illustrated in Figure 7 where a line is placed on top of the choke structure separated by a thin SiO_2 layer. The direct way to evaluate the efficiency of such a step in the ground plane is to observe what amount of the power is directed between the choke and the line and what fraction of the power remains trapped between the choke and the first ground plane. This would require to represent the structure as a 2 ports / 2 modes device. However to perform an electromagnetic simulation on such a structure is difficult and impractical since the thickness of the SiO_2 layer is much smaller (factor of 10^{-4}) compared to the choke dimensions. As a result the number of cells required to properly mesh the structure exceeds the workable amount of cells typical for a reasonable simulation. Therefore the SiO_2 layer and the transmission line are omitted in the

simulation and the choke is considered only as a band-stop filter with open ports. The performance of the above-defined structure is shown in Figure 8.

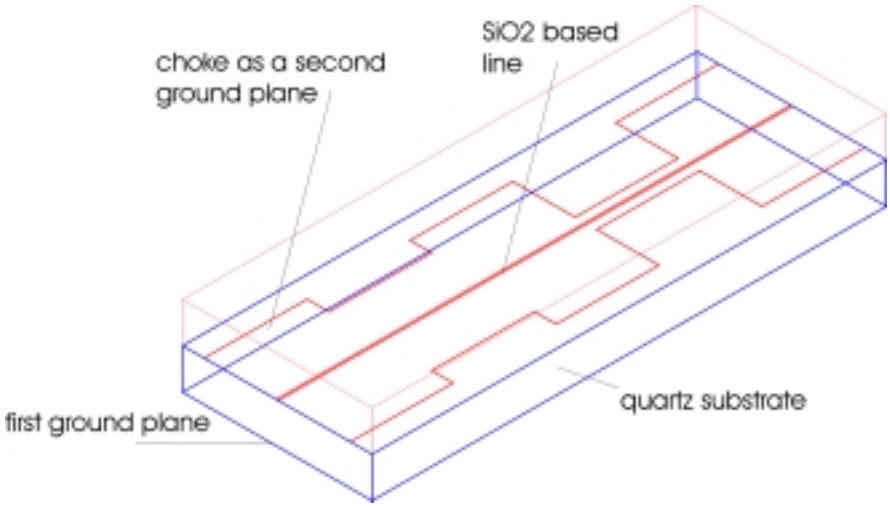

Figure 7 Choke structure on top of the quartz substrate and a line separated by a thin SiO_2 layer (not visible in the picture).

Since the ports of the choke are virtually short-circuited to the first ground plane (S_{11}, S_{22} in Figure 8) we can make the assumption that the power, which is not locked in between the choke and the first ground plane is directed between the choke and the transmission line. Therefore the loss, which is due to the step in the ground plane, should not exceed -3.10^{-3} dB (-22dB leak in the quartz substrate).

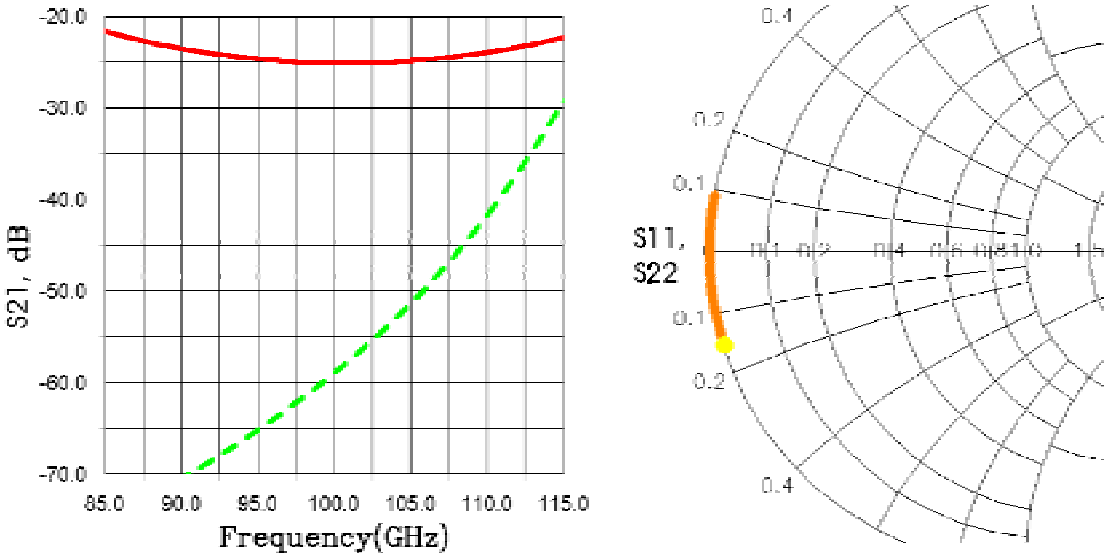

Figure 8 Transmission of the choke with open ports (terminated with the channel impedance) and the reflection at the ports. The solid line in the first plot represents the power in the main TEM mode, which remains trapped between the choke and the first ground plane, the dashed line illustrates the growth of the transverse resonant mode caused by the low impedance choke sections.

The dashed line in Figure 8 shows the appearance of the transverse resonant mode at ≈ 125 GHz, which restricts further increase of the width of the low impedance choke sections, the width of the high impedance sections is chosen to accommodate the SIS tuning circuitry.

LINE TRANSITION BETWEEN THE TWO DIELECTRICS

The line transition from 150 μm quartz to 400 nm SiO_2, as shown in Figure 9, creates significant geometrical and electrical discontinuity causing reflection even if the lines have identical impedances. Bringing the 'wide' quartz-based line close to the SiO_2 layer shunts the signal due to its excessive capacitance with respect to the 2nd ground plane. Different configurations of tapered shapes, to connect the two lines, were simulated to minimize the effect of the discontinuity. The distance *L* was optimized and for this particular example is about 30 μm.

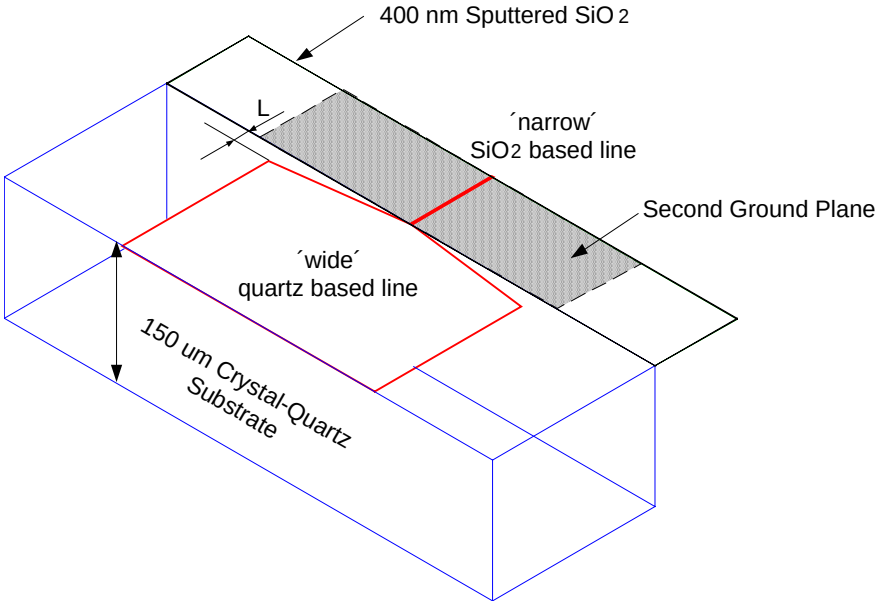

Figure 9 Quartz-based line to SiO_2-based line transition. Two lines having the same impedance but using dielectrics with different thickness are connected via a "tapered line" with optimized length.

In our simulations all the lines were modeled as perfect conductors, therefore the London penetration depth in a superconductor is not taken into account in the calculation of the line impedances. Therefore the actual line impedance exceeds the impedance computed by HFSS with factor of 1.15 for 400 nm SiO_2 substrate and line impedance of ≈ 30Ω. In other words a superconducting line having the same impedance as the line in HFSS would have been wider with a factor of 1.15. Nevertheless in terms of discontinuity this would not make any difference that may possibly affect the result of the simulation. The reflection produced by such a transition is presented in Figure 10.

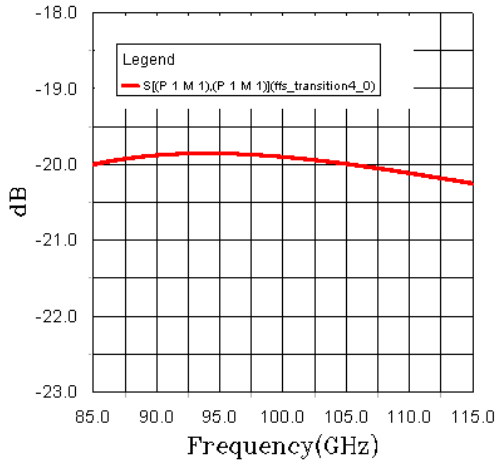

Figure 10 The reflection caused by the discontinuity in the line transition between quartz and SiO_2 dielectrics.

LO BRANCH LINE COUPLER

Finally to divide the LO power between the two mixers and to introduce the 90° phase difference a waveguide branch line coupler was designed. Since the required LO band is narrower compared to the RF band with 2 times the IF highest frequency, introducing the 90° phase difference in the LO path will benefit better phase and amplitude symmetry of the coupler due to the reduced bandwidth. To facilitate the machining the LO coupler (Figure 2) employs symmetrical branch sections [7].

The important parameters in the branch line coupler performance relevant for the image band isolation are the magnitude and the phase symmetry. Figure 11 shows the magnitude difference and the phase shift between the two channels.

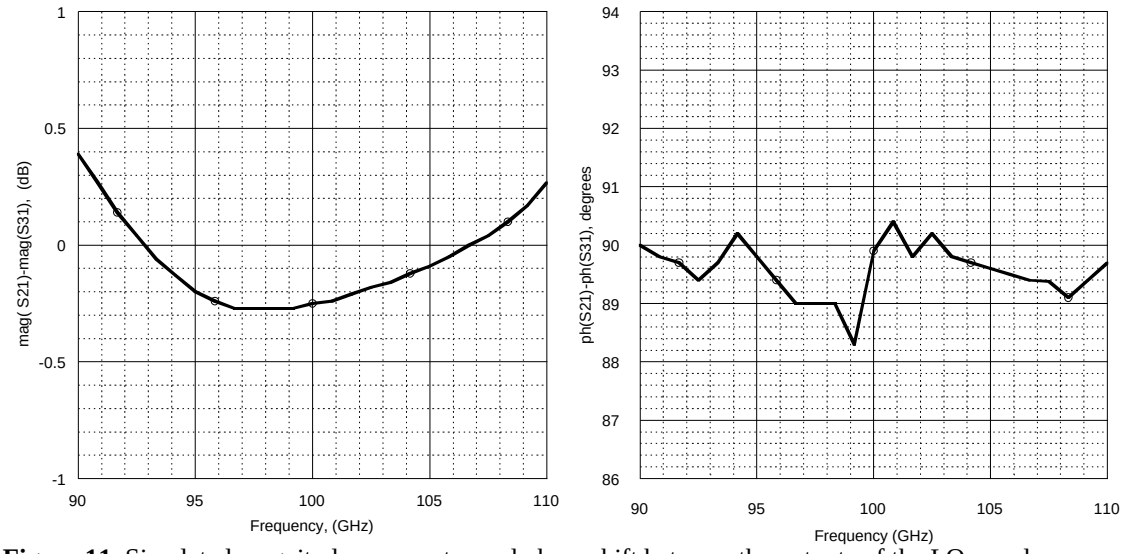

Figure 11 Simulated magnitude asymmetry and phase shift between the outputs of the LO coupler.

SIS INTEGRATED TUNING CIRCUIT

SIS junction tuning circuitry is designed using microstrip lines based on sputtered SiO_2 as a dielectric and consists of inductive section followed by an open stub (short circuit) as shown in Figure 12. This configuration is used for both SIS mixer junction and LO termination load and both circuits were optimized for source power match. Similar tuning circuitry was employed by [Carpenter] except we use the open stub input to connect DC bias and IF output.

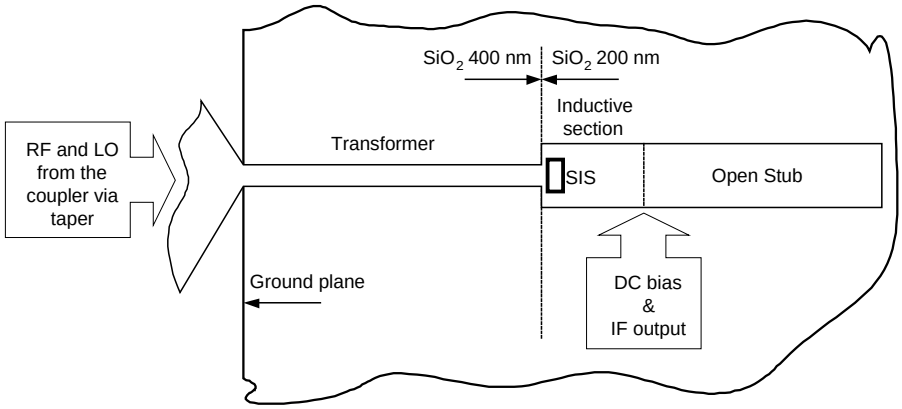

Figure 12 SIS tuning circuitry. This configuration is identical for both SIS mixer junctions and SIS LO termination junctions.

The mixer tuning was designed for source impedance of $\cong 69\Omega$ and frequency range 85 – 116 GHz. To provide matching between the SIS junction and the relatively high source impedance, the required transformer section impedance is of about $25\,\Omega$. In order to obtain the line with such impedance while keeping reasonable line dimensions we introduced a second 200 nm SiO_2 layer giving total dielectric thickness in the transformer section of ≈ 400 nm.

Using SIS junction with its tuning circuitry for LO termination gives the opportunity to produce it within the same processing steps as the mixer junction while the thin film resistors need additional and somewhat critical processing steps to achieve the required high resistivity of the normal metal film. The LO termination was optimized for the frequency band ΔF-$2F_{IF}$, where ΔF is the SIS mixer RF band (85 – 116 GHz) and F_{IF}=4.6 GHz is the upper intermediate frequency. The level of RF power at SIS junction is defined by parameter $\alpha = eV_{rf}/hf$, here **e** is the electron charge, **h** is Planck's constant and **f** is the operating frequency. The RF voltage across the LO termination junction, $\mathbf{V_{rf}}$, is 15 dB higher than the V_{rf} across the mixer junction (the coupling of the LO coupler is –15 dB). Assuming that the SIS mixer junction operates at α_m=1 at the SIS LO termination junction this will give $\alpha_t \approx 5$. The result of the circuit optimization is presented in Figure 13.

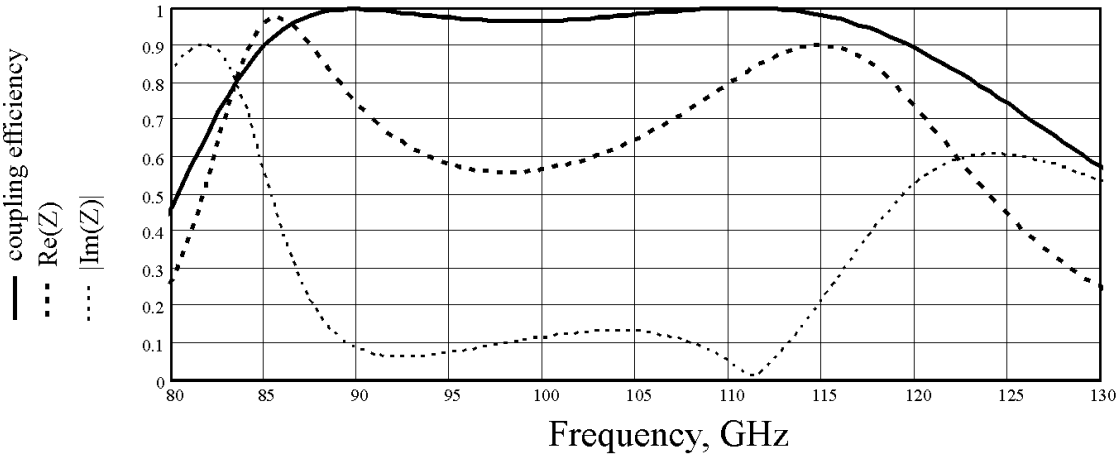

Figure 13 Coupling efficiency and impedance of the LO termination SIS junction together with its tuning circuitry. The values for the impedance are normalized to 69Ω which is the required impedance for matched LO coupler termination.

CONCLUSION

We present the design of a sideband separation mixer for 85-115 GHz. The mixer is based on a new device - a double-probe coupler, which makes possible the integration of all mixer components on the same compact substrate and thus ensures a high degree of similarity in the SIS junction performance and the geometry of all the mixer elements. Together with the good symmetry provided by the double-probe coupler and the LO branch line coupler, this gives the prospect of very good image band suppression.

REFERENCES

[1] Approach proposed by J. Kooi (private communication).
[2] P. R. Jewell, J. G. Mangum, "System Temperatures, Single Versus Double Sideband Operation, and Optimum Receiver Performance", MMA Memo. 170, National Radio Astronomy Observatory, Charlottesville VA, May, 1997.
[3] A. R. Kerr, S.-K. Pan and H. G. LeDuc, "*An integrated sideband separating SIS mixer for 200-280 GHz*", Proc. of the Ninth Space Terahertz Technology Symposium, Pasadena, USA, March, 1998.
[4] R. L. Akeson, J. E Carlstrom, D. P. Woody, J. Kawamura, A. R. Kerr, S. -K. Pan and K. Wan, "*Development of a Sideband Separation Receiver at 100GHz*", Proc of Fourth International Symposium on Space Terahertz Technology, pp.12-17, March, 1993.
[5] A. R. Kerr and S.-K. Pan, "*Design of Planar Image Separating and Balanced SIS Mixers*," Proc. of Seventh International Symposium on Space Terahertz Technology, March 12-14, 1996.
[6] V. Vassilev, V. Belitsky, Denis Urbain, S. Kovtonyuk, "*A New 3 dB Power Divider for MM-Wavelengths*" Accepted for publication in IEEE Microwave and Wireless Components Letters.
[7] S.M.X. Claude, C.T. Cunningham, A.R. Kerr, S.-K. Pan, "Design of a Sideband-Separating Balanced SIS Mixer Based on Waveguide Hybrids", ALMA Memo 316, http://www.alma.nrao.edu/memos.
[8] Agilent High Frequency Structure Simulator, HFSS, Agilent Technologies, 395 Page Mill Road, Paolo Alto, CA 94304, U.S.A.